

Supplementary Materials

Highly CO Selective Trimetallic Metal–Organic Framework Electrocatalyst for the Electrochemical Reduction of CO₂

Tran-Van Phuc, Jin-Suk Chung and Seung-Hyun Hur *

School of Chemical Engineering, University of Ulsan, Daehak-ro 93, Nam-gu, Ulsan 44610, Korea;
vanphuc0509@gmail.com (T.-V.P.); jschung@ulsan.ac.kr (J.-S.C.)

* Correspondence: shhur@ulsan.ac.kr

Table of contents

1. Faradaic efficiency.

2. Supplementary Figures and Tables

3. References

1. Faradaic efficiency calculation

$$FE = \frac{x_0 \times n \times N_A \times z}{\frac{I \times t}{e}}$$

FE: Faradaic Efficiency of the product / %

x₀: mole of the product detected by GC / mol

n: Total moles according to the ideal gas law ($\frac{P \times V}{R \times T}$), under ambient temperature experiment (25 °C)

z: Charge transfer of the product

N_A: Avogadro constant / mol⁻¹

I: total current through experiment

t: CO₂ gas flow rate / L s⁻¹

e: Electric charge / C

2. Supplementary figures and tables

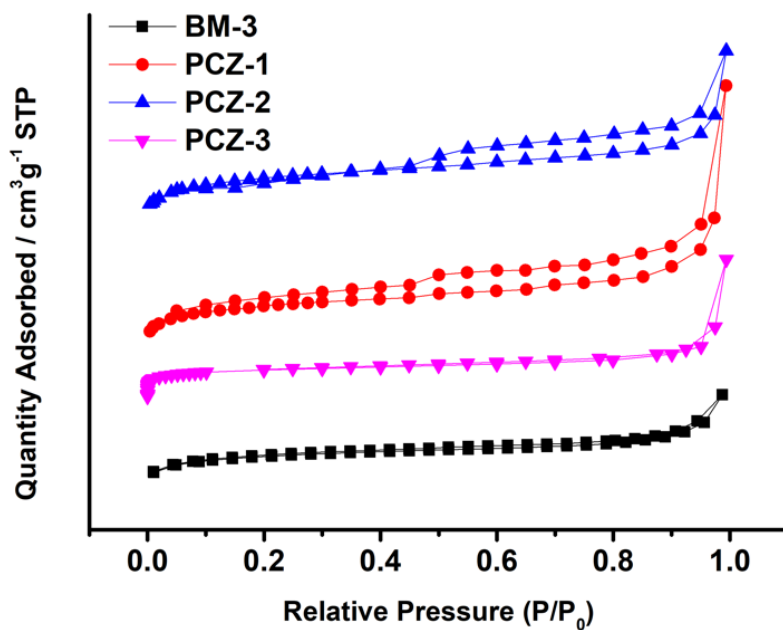
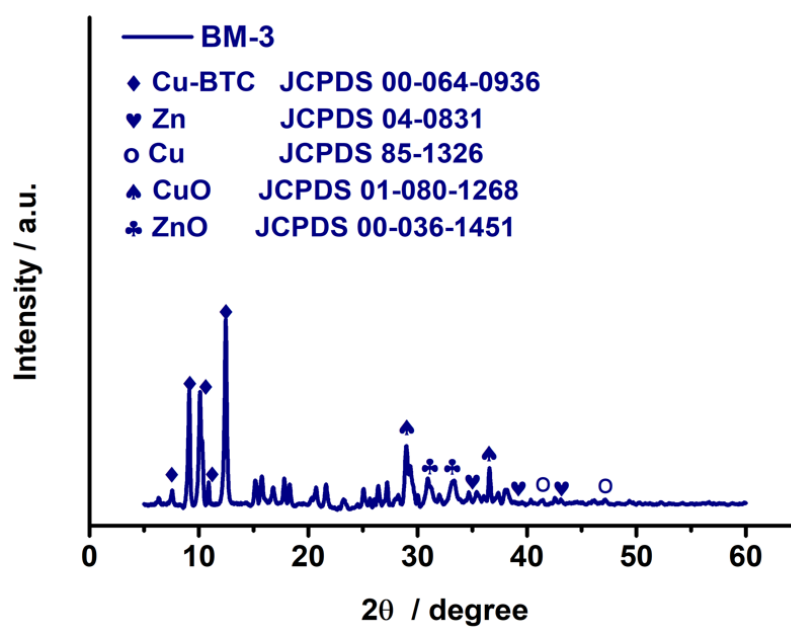
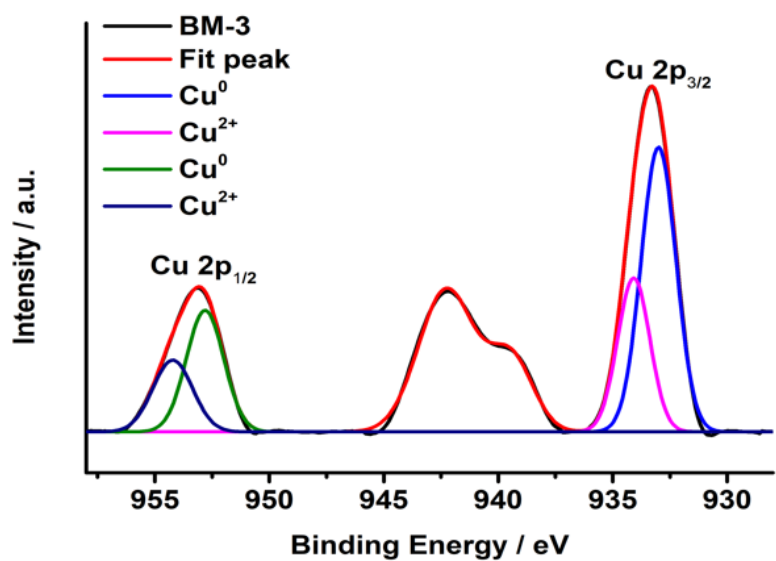
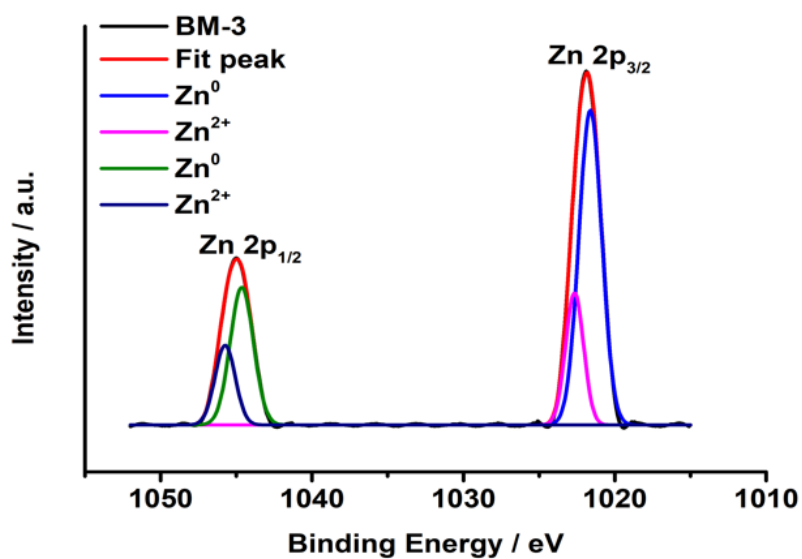
Figure S1. N₂ adsorption-desorption isothermal curves of PCZs and BM-3.

Figure S2. XRD patterns of BM-3.



(a)



(b)

Figure S3. The XPS spectra of (a) Cu 2p and (b) Zn 2p of BM-3.

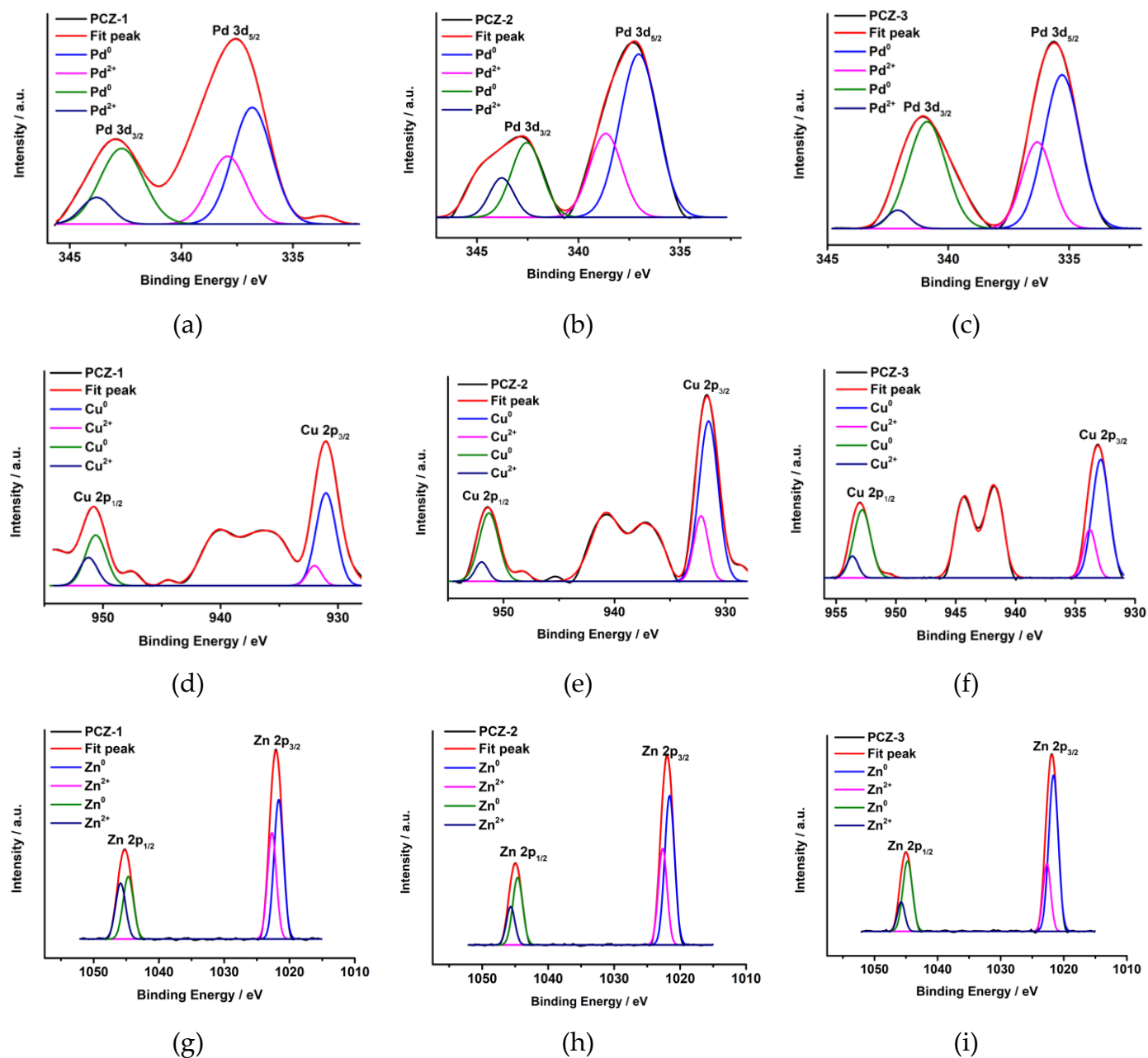


Figure S4. The XPS spectra Pd 3d, Cu 2p and Zn 2p of (a,d,g) PCZ-1, (b,e,h) PCZ-2, and (c,f,i) PCZ-3.

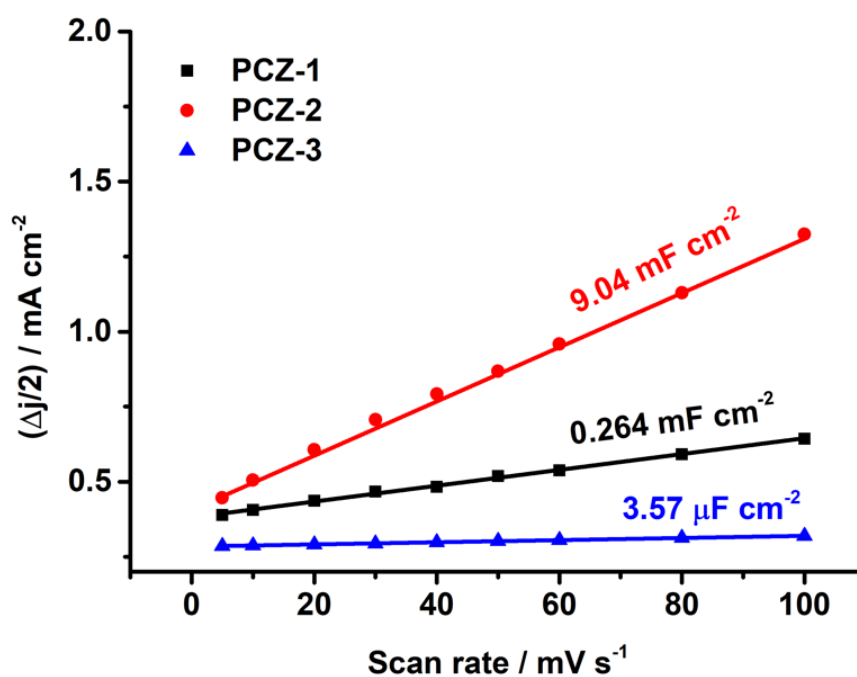


Figure S5. The measured capacitive currents as a function of scan rate for PCZs catalysts.

Calculated electrochemical active surface area, with $C_s = 0.029 \text{ mF cm}^{-2}$

PCZ-1:

$$A_{ECSA}^{PCZ-1} = \frac{0.264 \text{ mF cm}^{-2}}{29 \mu\text{F cm}^{-2} \text{ per cm}^2_{ECSA}} = 9.10 \text{ cm}^2_{ECSA}$$

PCZ-2:

$$A_{ECSA}^{PCZ-2} = \frac{9.04 \text{ mF cm}^{-2}}{29 \mu\text{F cm}^{-2} \text{ per cm}^2_{ECSA}} = 311.72 \text{ cm}^2_{ECSA}$$

PCZ-3:

$$A_{ECSA}^{PCZ-3} = \frac{3.57 \mu\text{F cm}^{-2}}{29 \mu\text{F cm}^{-2} \text{ per cm}^2_{ECSA}} = 0.123 \text{ cm}^2_{ECSA}$$

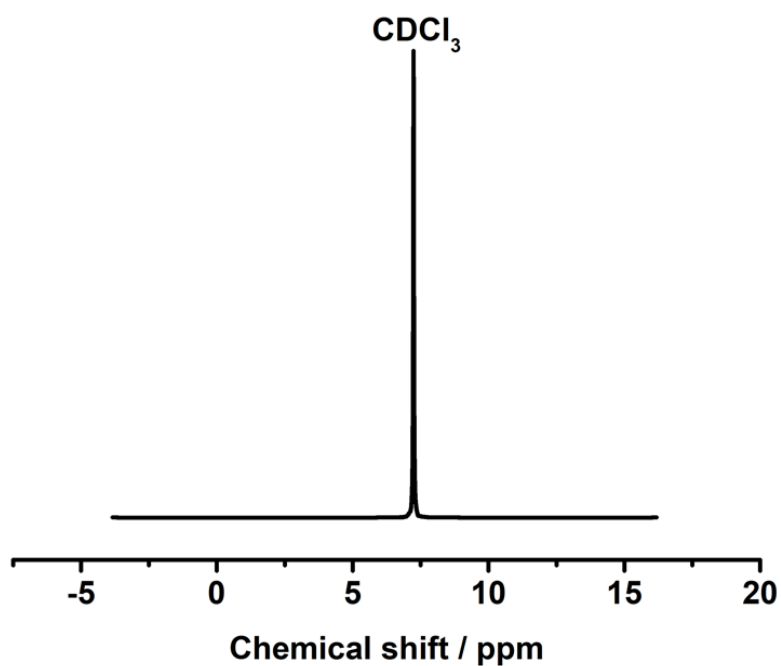


Figure S6. ^1H -NMR spectra of the electrolyte after CO_2 reduction electrolysis at -1.4 V vs. SCE for long-term test.

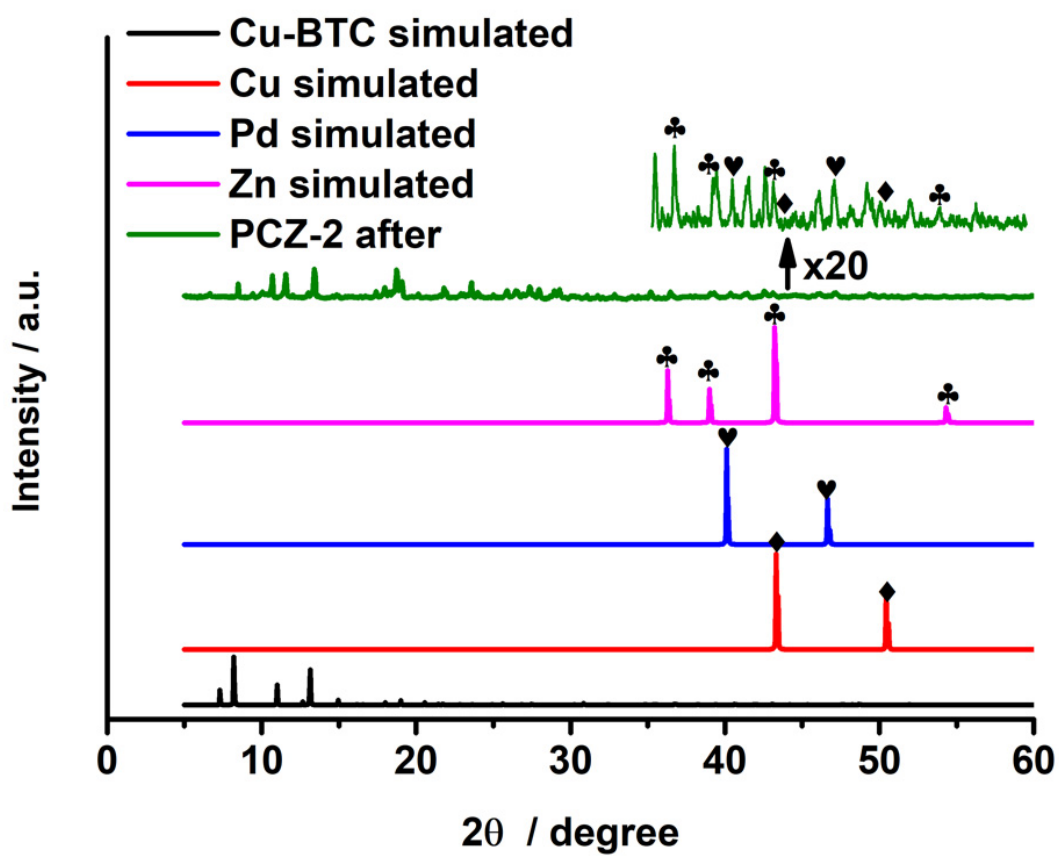


Figure S7. XRD patterns of PCZ-2 after long-term test.

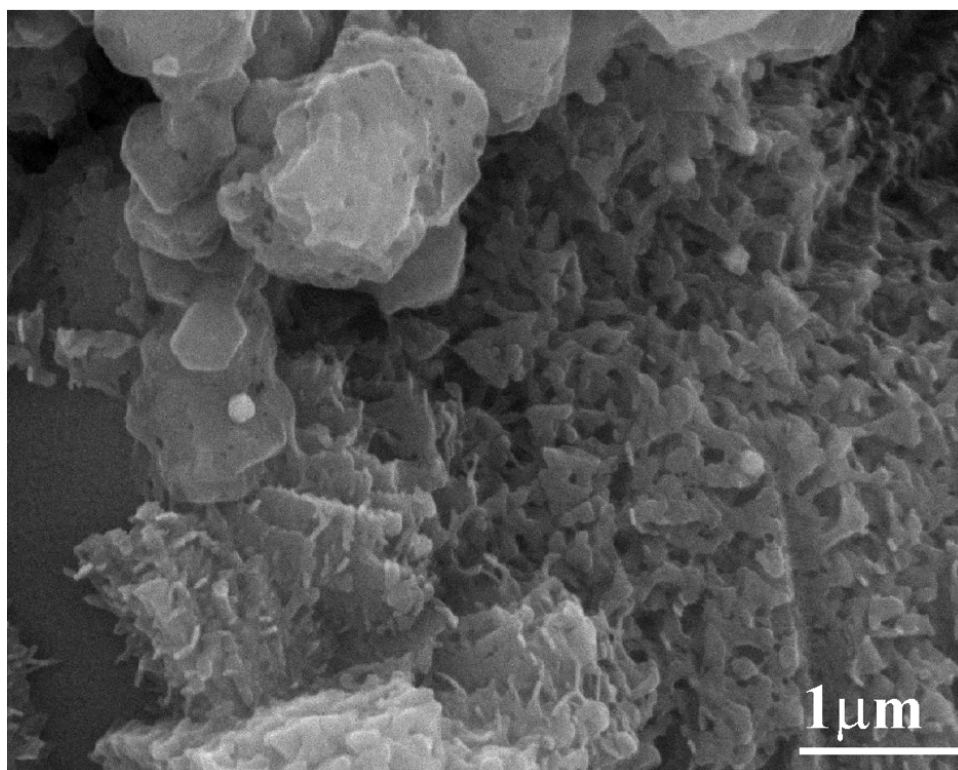
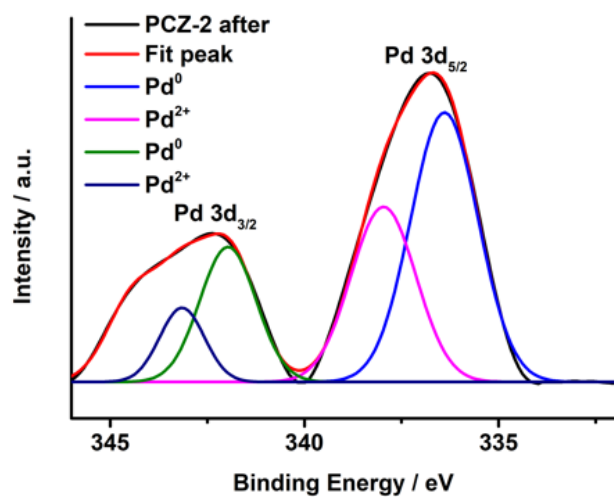
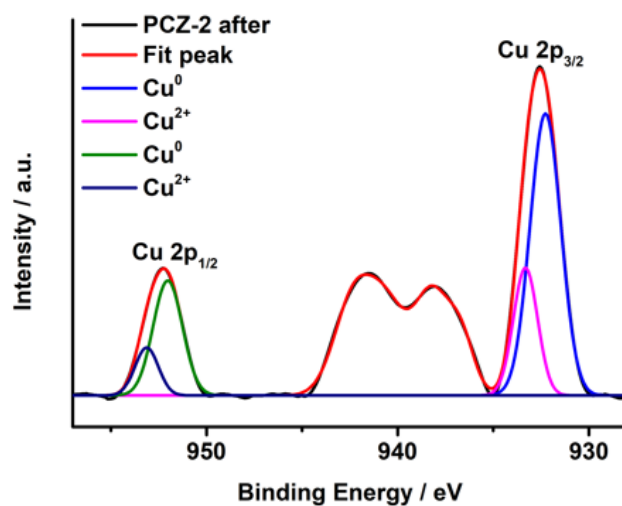


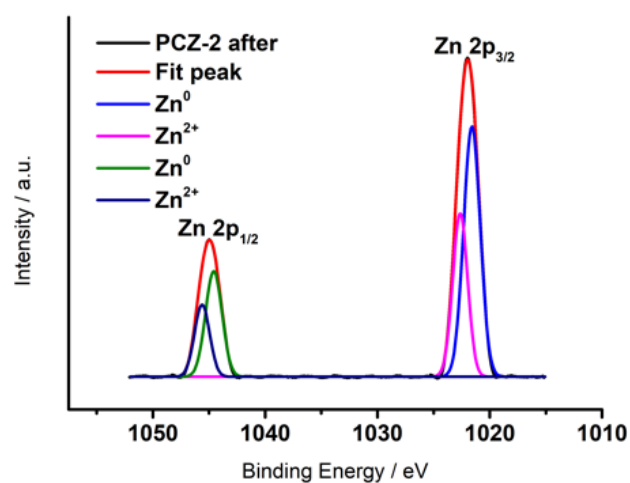
Figure S8. The SEM image of PCZ-2 after long-term test.



(a)



(b)



(c)

Figure S9. The XPS spectra of (a) Pd 3d, (b) Cu 2p and (c) Zn 2p of PCZ-2 after long-term test.

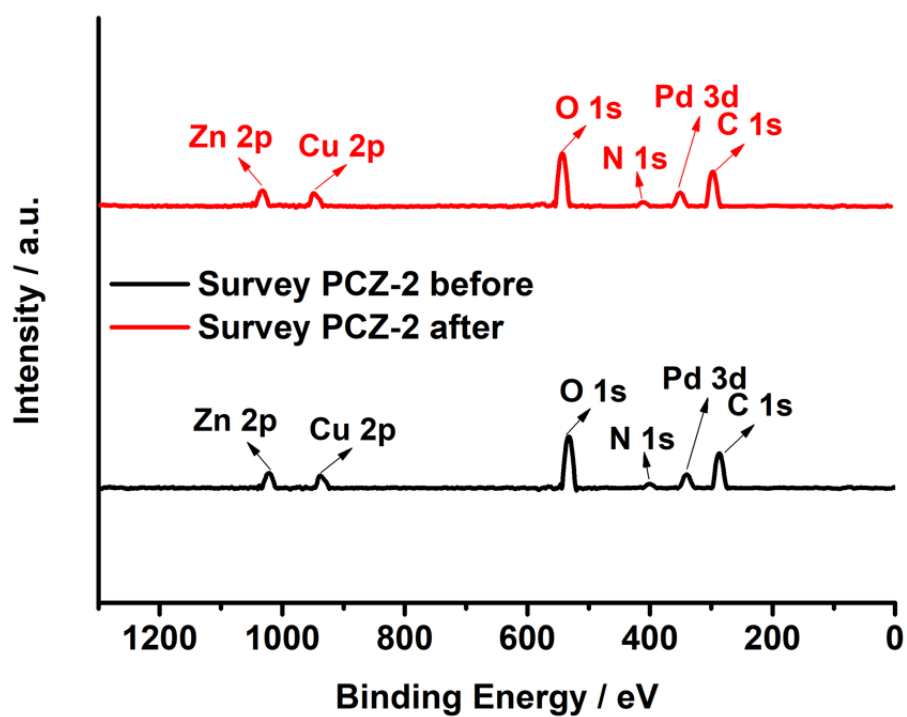


Figure S10. XPS survey spectra of PCZ-2 after long-term test.

Table S1. CO selectivity using among various catalysts.

Electrode	Electrolyte	FE _{CO} (%)	Applied Potential	<i>j</i> (mA.cm ⁻²)*	Reference
Cu-In	0.1 M KHCO ₃	85%	−0.60 V vs. RHE	>1	[1]
Pd ₈₅ Cu ₁₅ /C	0.1 M KHCO ₃	86%	−0.89 V vs. RHE	6.9	[2]
CuZn0.4	0.1 M KHCO ₃	70%	−1.0 V vs. RHE	4.3	[3]
ZIF-A-LD/CB	0.1 M KHCO ₃	75%	−1.0 V vs. RHE	3.2	[4]
2D c-MOF (PcCu-O ₈ -Zn)	0.1 M KHCO ₃	88%	−0.7 V vs. RHE	8	[5]
C-AFC@ZIF-8	1 M KHCO ₃	93%	−0.43 V vs. RHE	5.2	[6]
Ag ₂ O/layered ZIF	0.25 M K ₂ SO ₄	80.5%	−1.2 V vs. RHE	26.2	[7]
Cu-MOF74	0.1 M KHCO ₃	85%	−1.25 V vs. RHE	6.9	[8]
Zn ₉₄ Cu ₆ foam	0.5 M KHCO ₃	90%	−0.95 V vs. RHE	5	[9]
Co/Zn ZIF pyrolysis	0.5 M KHCO ₃	94%	−0.63 V vs. RHE	18.1	[10]
Cobalt-porphyrin MOF	0.5 M K ₂ CO ₃	76%	−0.70 V vs. RHE	~1	[11]
COF-367-Co(1%)	0.5 M KHCO ₃	90%	−0.67 V vs. RHE	1	[12]
PCZ-2	0.1 M KHCO ₃	95%	−0.75 V vs. RHE	3.99	This work

* *j* : refers to geometric current density or partial current density with specific subscript.

Table S2. Surface area and pore size of PCZ-n (n= 1-3) and BM-3 samples.

Sample	Surface area (m ² /g)	Pore volume (cm ³ /g)	Pore size (nm)
PCZ-1	126.11	0.32	2.4
PCZ-2	271.40	0.45	4.5
PCZ-3	40.74	0.11	10.8
BM-3	22.15	0.11	20.47

3. Reference

1. Rasul, S.; Anjum, D.H.; Jedidi, A.; Minenkov, Y.; Cavallo, L.; Takanabe, K. A Highly Selective Copper–Indium Bimetallic Electrocatalyst for the Electrochemical Reduction of Aqueous CO₂ to CO. *Angew. Chem. Int. Ed.* **2015**, *54*, 2146–2150, doi:10.1002/anie.201410233.
2. Yin, Z.; Gao, D.; Yao, S.; Zhao, B.; Cai, F.; Lin, L.; Tang, P.; Zhai, P.; Wang, G.; Ma, D.; et al. Highly selective palladium-copper bimetallic electrocatalysts for the electrochemical reduction of CO₂ to CO. *Nano Energy* **2016**, *27*, 35–43, doi:https://doi.org/10.1016/j.nanoen.2016.06.035.
3. Zeng, J.; Rino, T.; Bejtka, K.; Castellino, M.; Sacco, A.; Farkhondehfal, M.A.; Chiodoni, A.; Drago, F.; Pirri, C.F. Coupled Copper–Zinc Catalysts for Electrochemical Reduction of Carbon Dioxide. *ChemSusChem* **2020**, *13*, 4128–4139, doi:https://doi.org/10.1002/cssc.202000971.
4. Dou, S.; Song, J.; Xi, S.; Du, Y.; Wang, J.; Huang, Z.-F.; Xu, Z.J.; Wang, X. Boosting Electrochemical CO₂ Reduction on Metal–Organic Frameworks via Ligand Doping. *Angew. Chem. Int. Ed.* **2019**, *58*, 4041–4045, doi:https://doi.org/10.1002/anie.201814711.
5. Zhong, H.; Ghorbani-Asl, M.; Ly, K.H.; Zhang, J.; Ge, J.; Wang, M.; Liao, Z.; Makarov, D.; Zschech, E.; Brunner, E.; et al. Synergistic electroreduction of carbon dioxide to carbon monoxide on bimetallic layered conjugated metal-organic frameworks. *Nat. Commun.* **2020**, *11*, 1409, doi:10.1038/s41467-020-15141-y.
6. Ye, Y.; Cai, F.; Li, H.; Wu, H.; Wang, G.; Li, Y.; Miao, S.; Xie, S.; Si, R.; Wang, J.; et al. Surface functionalization of ZIF-8 with ammonium ferric citrate toward high exposure of Fe-N active sites for efficient oxygen and carbon dioxide electroreduction. *Nano Energy* **2017**, *38*, 281–289, doi:https://doi.org/10.1016/j.nanoen.2017.05.042.
7. Jiang, X.; Wu, H.; Chang, S.; Si, R.; Miao, S.; Huang, W.; Li, Y.; Wang, G.; Bao, X. Boosting CO₂ electroreduction over layered zeolitic imidazolate frameworks decorated with Ag₂O nanoparticles. *J. Mater. Chem. A* **2017**, *5*, 19371–19377, doi:10.1039/C7TA06114E.
8. Van Phuc, T.; Kang, S.G.; Chung, J.S.; Hur, S.H. Highly selective metal-organic framework-based electrocatalyst for the electrochemical reduction of CO₂ to CO. *Mater. Res. Bull.* **2021**, *138*, 111228, doi:https://doi.org/10.1016/j.materresbull.2021.111228.
9. Moreno-García, P.; Schlegel, N.; Zanetti, A.; Cedeño López, A.; Gálvez-Vázquez, M.d.J.; Dutta, A.; Rahaman, M.; Broekmann, P. Selective Electrochemical Reduction of CO₂ to CO on Zn-Based Foams Produced by Cu²⁺ and Template-Assisted Electrodeposition. *ACS Appl. Mater. Interfaces* **2018**, *10*, 31355–31365, doi:10.1021/acsami.8b09894.
10. Wang, X.; Chen, Z.; Zhao, X.; Yao, T.; Chen, W.; You, R.; Zhao, C.; Wu, G.; Wang, J.; Huang, W.; et al. Regulation of Coordination Number over Single Co Sites: Triggering the Efficient Electroreduction of CO₂. *Angew. Chem. Int. Ed.* **2018**, *57*, 1944–1948, doi:10.1002/anie.201712451.
11. Kornienko, N.; Zhao, Y.; Kley, C.S.; Zhu, C.; Kim, D.; Lin, S.; Chang, C.J.; Yaghi, O.M.; Yang, P. Metal–Organic Frameworks for Electrocatalytic Reduction of Carbon Dioxide. *J. Am. Chem. Soc.* **2015**, *137*, 14129–14135, doi:10.1021/jacs.5b08212.
12. Lin, S.; Diercks, C.S.; Zhang, Y.-B.; Kornienko, N.; Nichols, E.M.; Zhao, Y.; Paris, A.R.; Kim, D.; Yang, P.; Yaghi, O.M.; et al. Covalent organic frameworks comprising cobalt porphyrins for catalytic CO₂ reduction in water. *Science* **2015**, *349*, 1208, doi:10.1126/science.aac8343.